2nd URSI AT-RASC, Gran Canaria, 28 May – 1 June 2018

Repeatability Investigation of BeiDou Receiver Differential Code Bias

Mohamed Abdelazeem (1)
(1) Civil Engineering Department, Faculty of Engineering, Aswan University, Egypt

Abstract

Currently, the Chinese BeiDou satellite system is extensively used in ionosphere modeling and space weather applications. For precise ionosphere modeling, however, the differential code bias (DCB) for both the satellite and receiver must be accounted for. The objective of this paper is to investigate the repeatability of the BeiDou receiver DCB. GPS/BeiDou observations from a number of globally distributed stations over a period of 7 days are used. The stations are selected from different latitudes in order to reflect different ionospheric characteristics. The observations are processed in the zero-differenced mode. The single-station bi-linear expansion is used in order to model the vertical total electron content (VTEC), the satellite and the receiver differential code biases. The findings indicate that the BeiDou receiver DCB has repeatability with level less than 0.8 ns. Then, the estimated DCB values are compared with the international GNSS service multi-GNSS experiment (IGS-MGEX) counterpart. The results show that the BeiDou receiver DCB has good agreement with the IGS-MGEX counterpart with mean difference and standard deviation (STD) values less than 0.7 ns.

1. Introduction

The Chinese BeiDou satellite system is currently used in modeling the spatial and temporal resolution of the ionosphere vertical total electron content (VTEC). To precisely model the VTEC, however, the differential code bias (DCB) for both the satellite and the receiver must be accounted for. Differential code bias is the difference in code hardware delays at two different frequencies. The satellite DCB values are stable over one day, while the receiver DCBs are not as stable [1]. Therefore, modeling the variation of the receiver DCB is crucial issue.

More recently, the estimation of the BeiDou DCB has been investigated by a number of researchers e.g., [2, 3, 4, 5, 6 and 7]. [6] developed a model to estimate the multi-constellation global navigation satellite systems (multi-GNSS) satellite and receiver DCBs. In their model, the local ionosphere was modeled using the generalized triangular series instead of the global ionospheric model. The DCBs estimated from their model showed good agreement with the center for orbit determination in Europe (CODE) and German aerospace center (DLR) counterparts. The stability of the GNSS receiver differential code bias has been investigated in a number of studies e.g., [8, 9, 10, 11 and 12]. [12] developed a model to estimate the multi-GNSS receiver DCB using the international GNSS service (IGS) global ionospheric map and the DLR satellite DCBs within 1-hour time resolution. Then, the short-term variation (i.e., intra-day) of the estimated DCBs was investigated. It has shown that the estimated receiver DCBs had good agreement with the DLR counterpart. In addition, there were large fluctuations between two consecutive hours within the receiver DCBs.

In this study, the repeatability of the BeiDou receiver DCB is investigated. GPS/BeiDou observations from a number of globally distributed reference stations are used. To reflect different ionospheric characteristics the stations are selected from different latitudes. The observations are processed in the zero-differenced mode. In order to estimate the VTEC, the satellite and the receiver DCBs, the single-station bi-linear expansion function is used. The BeiDou receiver DCBs are estimated over a period of 7 days, which is corresponding to different geomagnetic activity and solar activity. Thereafter, the estimated receiver DCBs are compared with the IGS multi-GNSS experiment (IGS-MGEX) counterpart. It is shown that the repeatability of the difference between the estimated receiver DCB and the IGS-MGEX is less than 1.2 ns.

2. Development of BeiDou Receiver DCB Estimation Model

The basic GNSS code observations can be written as follows [13]:

$$P_{G1} = \rho_r^G + c(dt_r - dt^G) + I_{r,1}^G + T_r^G + c\left(d_{r,1} + d_1^G\right) + \varepsilon_{G,p,1} \quad (1)$$
$$P_{G2} = \rho_r^G + c(dt_r - dt^G) + I_{r,2}^G + T_r^G + c\left(d_{r,2} + d_2^G\right) + \varepsilon_{G,p,2} \quad (2)$$
$$P_{B1} = \rho_r^B + c(dt_r - dt^B) + I_{r,1}^B + T_r^B + c\left(d_{r,1} + d_1^B\right) + \varepsilon_{B,p,1} \quad (3)$$
$$P_{B2} = \rho_r^B + c(dt_r - dt^B) + I_{r,2}^B + T_r^B + c\left(d_{r,2} + d_2^B\right) + \varepsilon_{B,p,2} \quad (4)$$

where G and B refer to the GPS and BeiDou satellite systems, respectively; P_{G1} and P_{G2} are the GPS pseudorange measurements on L1 and L2, respectively; P_{B1} and P_{B2} are the BeiDou pseudorange measurements on B1 and B2, respectively; ρ_r^G and ρ_r^B are the satellite-receiver true geometric ranges; c is the speed of light in vacuum; $I_{r,1}^G$ and $I_{r,2}^G$ are the ionospheric delay on L1 and L2, respectively; $I_{r,1}^B$ and $I_{r,2}^B$ are the ionospheric delay on B1 and B2, respectively; T_r^G and T_r^B are the tropospheric delay for the GPS and BeiDou systems, respectively; d_r is the code hardware delay for the receiver; d^G and d^B are the code hardware delay for the GPS and BeiDou satellites, respectively; ε_p is the code unmodeled errors, including noise and multipath.

The geometry-free linear combinations are used in order to remove the geometrical term, tropospheric delay, receiver and satellite clock errors from the zero-differenced smoothed code observations as follows [14]:

$$P_{4G} = P_{\tilde{G1}} - P_{\tilde{G2}}, \qquad P_{4B} = P_{\tilde{B1}} - P_{\tilde{B2}} \tag{5}$$

$$P_{4G} = MF \times k_G \times VTEC + c\left(d_{r,1} - d_{r,2}\right) + c(d_1^G - d_2^G) \tag{6}$$

$$P_{4B} = MF \times k_B \times VTEC + c\left(d_{r,1} - d_{r,2}\right) + c(d_1^B - d_2^B) + ISB \tag{7}$$

where $P_{\tilde{G1}}, P_{\tilde{G2}}, P_{\tilde{B1}}$ and $P_{\tilde{B2}}$ are the smoothed code observations of the GPS and BeiDou systems, respectively; P_{4G} and P_{4B} are the geometry free combination of the GPS and BeiDou smoothed code observations, respectively; MF is the mapping function; k_G and k_B are frequency-dependent factors for the GPS and BeiDou systems, respectively; ISB is the geometry-free inter-system bias between the GPS and BeiDou systems, which is the difference in code hardware delay between the GPS and BeiDou signals in the receiver channels. The inter-system bias is lumped into the receiver differential code bias for the BeiDou signals. Therefore, the geometry-free formulas can be rewritten as follows:

$$P_{4G} = MF \times k_G \times VTEC + cDCB_{r,G} + cDCB^G \tag{8}$$

$$P_{4B} = MF \times k_B \times VTEC + cDCB_{r,B} + cDCB^B \tag{9}$$

where DCB^G and DCB^B are the differential code bias for the GPS and the BeiDou satellites, respectively; $DCB_{r,G}$ and $DCB_{r,B}$ are the receiver differential code bias for the GPS and the BeiDou systems, respectively. The frequency-dependent factor k can be written as follows:

$$k_G = \frac{40.3(f_{G1}^2 - f_{G2}^2)}{(f_{G1}^2 f_{G2}^2)}, \quad k_B = \frac{40.3(f_{B1}^2 - f_{B2}^2)}{(f_{B1}^2 f_{B2}^2)} \tag{10}$$

where f_{G1} and f_{G2} are the carrier phase frequencies on L_1 and L_2 GPS signals, respectively; f_{B1} and f_{B2} are the carrier phase frequencies on B_1 and B_2 BeiDou signals, respectively. The mathematical expression for the mapping function can be written as follows [14]:

$$MF = \left[cos\left(arcsin\left(\frac{R}{R+H} sin(z)\right)\right)\right]^{-1} \tag{11}$$

where z is the satellite's zenith distance at receiver; R is the mean radius of the Earth, and H is the height of ionosphere thin shell layer.

The vertical TEC can be modeled over each station using the first-order bilinear expansion function depending upon the ionosphere pierce point (IPP) coordinates and time, which takes the form [15 and 16]:

$$VTEC = a_0 + a_1 \times d\lambda + a_2 \times d\varphi \tag{12}$$

where $VTEC$ is the ionospheric observable; a_0, a_1 and a_2 are the bi-linear expansion parameters; $d\lambda = \lambda_{IPP} - \lambda_R$ is the difference between the longitude of the IPP and the longitude of the receiver, and $d\varphi = \varphi_{IPP} - \varphi_R$ is the difference between the latitude of the IPP and the latitude of the receiver.

Substituting Equation 12 into Equations 8 and 9, the ionospheric bi-linear expansion model can be rewritten as follows:

$$P_{4G} = MF \times k_G \times [a_0 + a_1 \times d\lambda + a_2 \times d\varphi] + cDCB_{r,G} + cDCB^G \tag{13}$$

$$P_{4B} = MF \times k_B \times [a_0 + a_1 \times d\lambda + a_2 \times d\varphi] + cDCB_{r,B} + cDCB^B \tag{14}$$

where $a_0, a_1, a_2, DCB_{r,G}$ and are $DCB_{r,B}$ the unknown parameters to be determined. The GPS and BeiDou satellite DCB (i.e., DCB^G, DCB^B) are obtained from the publicly available MGEX file [17].

To calculate the unknown VTEC parameters and receiver DCBs, a weighted least-squares algorithm is developed as follows:

$$\boldsymbol{x} = (\boldsymbol{A^T P A})^{-1} \boldsymbol{A^T P l} \tag{15}$$

where the matrices of $\boldsymbol{x}, \boldsymbol{A}$ and $\boldsymbol{l}$ are expressed as follows:

$$\boldsymbol{x} = \begin{bmatrix} a_0 \\ a_1 \\ a_2 \\ DCB_{r,G} \\ DCB_{r,B} \end{bmatrix}, \boldsymbol{l} = \begin{bmatrix} (P_{4G} - c \times DCB^{G=1}) \\ \vdots \\ (P_{4G} - c \times DCB^{G=n_G}) \\ (P_{4B} - c \times DCB^{B=1}) \\ \vdots \\ (P_{4B} - c \times DCB^{B=n_B}) \end{bmatrix}, \tag{16}$$

$$\boldsymbol{A} = \begin{bmatrix} (MF \times k_G) & (MF \times k_B \times d\lambda)^{G=1} & (MF \times k_B \times d\varphi)^{G=1} & 1 & 0 \\ \vdots & \vdots & \vdots & \vdots & \vdots \\ (MF \times k_G) & (MF \times k_B \times d\lambda)^{G=n_G} & (MF \times k_B \times d\varphi)^{G=n_G} & 1 & 0 \\ (MF \times k_B) & (MF \times k_B \times d\lambda)^{B=1} & (MF \times k_B \times d\varphi)^{B=1} & 0 & 1 \\ \vdots & \vdots & \vdots & \vdots & \vdots \\ (MF \times k_B) & (MF \times k_B \times d\lambda)^{B=n_B} & (MF \times k_B \times d\varphi)^{B=n_B} & 0 & 1 \end{bmatrix}$$

where $DCB_{r,G}$ and $DCB_{r,B}$ are the receiver differential code bias for the GPS and BeiDou systems, respectively; n_G and n_B are the number of GPS and BeiDou satellites, respectively, in a single observation epoch. For the weight matrix ($\boldsymbol{P}$), the elevation-dependent weighting of the observations is used.

3. Methodology

To develop the aforementioned receiver DCB estimation model, four globally distributed IGS-MGEX reference stations are used (Figure 1). The stations are selected to represent different latitudes in order to reflect different ionosphere characteristics. In addition, the stations are occupied with different receiver types (Table 1). GPS/BeiDou observations over 7 days (day of year (DOY) 225 to 231 in 2017) are downloaded [18].

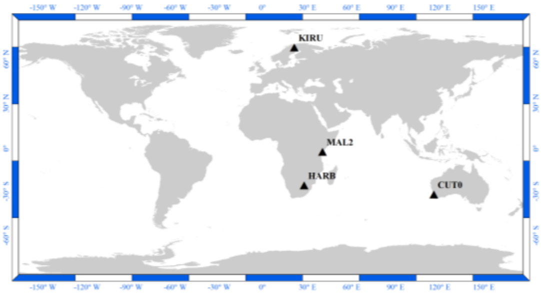

Figure 1. Examined stations distributions

Table 1. Examined station properties

Station	Latitude	Longitude	Receiver type
KIRU	67.8574º	20.9684º	Sept Polarx4
MAL2	-2.9960º	40.194º	Sept Polarx4
HARB	-25.8869º	27.7072º	Trimble Netr9
CUT0	-32.0038º	115.8947º	Trimble Netr9

The solar activity ($F_{10.7cm}$) and the geomagnetic activity (A_p) indices over the examined days are given in Table 2. It is shown that the solar activity is low over the examined days, while the geomagnetic is quiet in the first four days and active in the last three examined days.

Table 2. $F_{10.7}$ and A_P indices for the examined days [19]

DOY	$F_{10.7\ cm}$	A_P	DOY	$F_{10.7\ cm}$	A_P
225	70	6	229	78.5	24
226	74.9	4	230	82	20
227	76.1	2	231	88.9	29
228	79.2	5			

Each observation file has a 30-second time interval in RINEX 3.02 format. The elevation cut-off angle is selected to be 10º. The observation files are processed in the zero-difference mode. The geometry-free linear combination is formed using the smoothed code observations (i.e., $P_{\widetilde{G1}}, P_{\widetilde{G2}}, P_{\widetilde{B1}}$ and $P_{\widetilde{B2}}$). For the ionospheric mapping function, the effective height (H) is selected to be 450 km. The final IGS-MGEX satellite orbit and clock products are used [20]. For the least-squares estimation (Eqs.15 and 16), the extracted satellite DCBs from the MGEX file [17] are used. The receiver DCBs are determined every 1-hour time interval. The proposed model is implemented in FORTRAN computer code by the author.

4. Results and Analysis

In order to evaluate the developed model, the standard deviation (STD) of the estimated receiver DCBs are given in Figure 2. It is shown that the STD of the BeiDou receiver DCB is less than 4 ns. In addition, the STD values at station MAL2 is larger than other stations. This can be attributed to the fact that station MAL2 is located at the equatorial region. On the other hand, the STD values at station CUT0 is slightly smaller than the others. This might be attributed to the station's location, which is at a mid-latitude region.

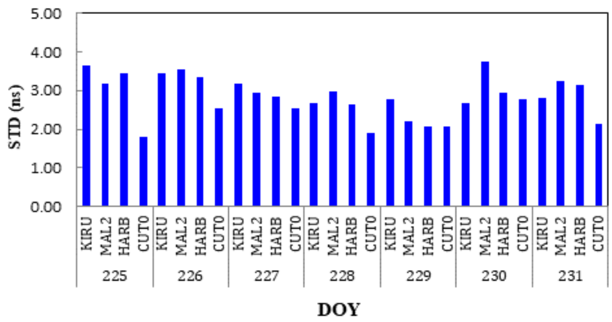

Figure 2. STD of the estimated BeiDou receiver DCBs

In order to assess the repeatability of the estimated BeiDou receiver differential code bias, the average DCB over each day is computed. Then, the STD for the differences between two successive days is estimated. Figure 3 illustrates the repeatability of the estimated BeiDou receiver differential code bias. It can be seen that the repeatability of the BeiDou DCB is less than 0.8 ns.

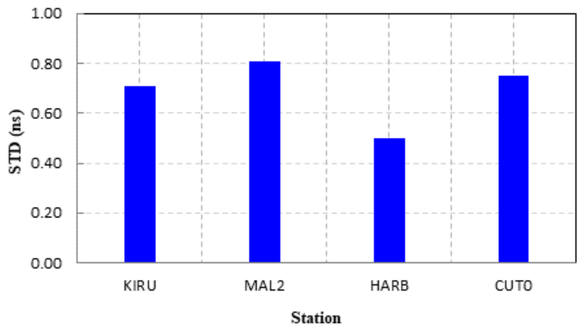

Figure 3. Repeatability of the estimated DCBs

Moreover, to evaluate the accuracy of the developed model, the estimated receivers DCB are compared with the IGS-MGEX counterparts. The mean difference and the STD values over the examined days are given in Table 3.

Table 3. Mean difference and STD values

Station	Mean (ns)	STD (ns)
KIRU	0.16	±0.54
MAL2	-0.45	±0.63
HARB	-0.39	±0.45
CUT0	-0.58	±0.44

It is seen that the estimated BeiDou receiver DCB show good agreement with the IGS-MGEX with mean difference and STD values less than 0.7 ns. Additionally, the repeatability errors of the estimated DCB with respect to the IGS-MGEX are calculated (Figure 4). It can be seen that the repeatability error of the BeiDou DCB in comparison with the IGS-MGEX is less than 1.2 ns. Also, station MAL2 has the largest value as it is located at equatorial region.

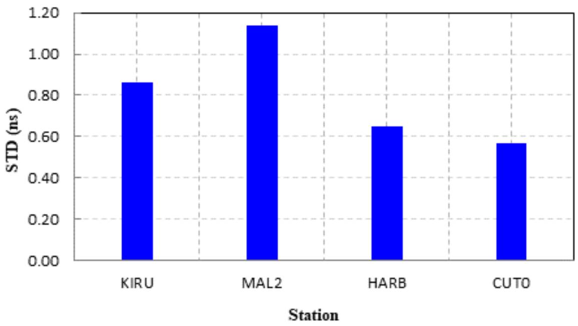

Figure 4. Repeatability error of the estimated DCBs with respect to the IGS-MGEX

5. Conclusion

In this study, the repeatability of the BeiDou receiver differential code bias has been investigated. GPS/BeiDou observations from four globally distributed IGS-MGEX reference stations have been used. The stations have been selected with different latitudes and receiver types. The observations have been processed in the zero-differenced mode. The bi-linear function has been used in order to estimate the receiver DCB. The DCBs have been estimated over a period of 7 days with different geomagnetic activity. The results show the BeiDou receiver DCB has repeatability level less than 0.8 ns. Moreover, the estimated DCB is compared with the IGS-MGEX counterpart. It has shown the estimated DCB agree with the IGS-MGEX with mean difference and STD values less than 0.7 ns. In addition, the repeatability of the difference between the estimated receiver DCB and the IGS-MGEX is less than 1.2 ns.

6. References

[1] S. Schaer, "Mapping and Predicting the Earth's Ionosphere Using the Global Positioning System," PhD Thesis, University of Bern, Switzerland, 1999.
[2] Z. Li, Y. Yuan, H. Li, J. Ou, and X. Huo, "Two-step method for the determination of the differential code biases of COMPASS satellites," Journal of Geodesy, vol. 86, pp. 1059-1076, 2012.
[3] O. Montenbruck, A. Hauschild, and P. Steigenberger, "Differential Code Bias Estimation using Multi-GNSS Observations and Global Ionosphere Maps, " Institute of Navigation International Technical Meeting, San Diego, CA, United States, 802–812, 2014.
[4] Z. Li, Y. Yuan, L. Fan, X. Huo, and H. Hsu, "Determination of the Differential Code Bias for Current BDS Satellites," IEEE Transactions on Geoscience and Remote Sensing, vol. 52, pp. 3968-3979, 2014.
[5] M. Abdelazeem, R. N. Çelik, and A. El-Rabbany, "MGR-DCB: A Precise Model for Multi-Constellation GNSS Receiver Differential Code Bias," Journal of Navigation, vol. 69, pp. 698-708, 2015.
[6] N. Wang, Y. Yuan, Z. Li, O. Montenbruck, and B. Tan, "Determination of differential code biases with multi-GNSS observations," Journal of Geodesy, vol. 90, pp. 209-228, 2015.
[7] C. Shi, L. Fan, M. Li, Z. Liu, S. Gu, S. Zhong, et al., "An enhanced algorithm to estimate BDS satellite's differential code biases," Journal of Geodesy, vol. 90, pp. 161-177, 2015.
[8] D. H. Zhang, W. Zhang, Q. Li, L. Q. Shi, Y. Q. Hao, and Z. Xiao, "Accuracy analysis of the GPS instrumental bias estimated from observations in middle and low latitudes," Annales Geophysicae, vol. 28, pp. 1571-1580, 2010.
[9] D. Zhang, H. Shi, Y. Jin, W. Zhang, Y. Hao, and Z. Xiao, "The variation of the estimated GPS instrumental bias and its possible connection with ionospheric variability," Science China Technological Sciences, vol. 57, pp. 67-79, 2013.
[10] J. Xue, S. Song, and W. Zhu, "Estimation of differential code biases for Beidou navigation system using multi-GNSS observations: How stable are the differential satellite and receiver code biases?," Journal of Geodesy, vol. 90, pp. 309-321, 2015.
[11] J. Sanz, J. Miguel Juan, A. Rovira-Garcia, and G. González-Casado, "GPS differential code biases determination: methodology and analysis," GPS Solutions, vol. 21, pp. 1549-1561, 2017.
[12] M. Li, Y. Yuan, N. Wang, T. Liu, and Y. Chen, "Estimation and analysis of the short-term variations of multi-GNSS receiver differential code biases using global ionosphere maps," Journal of Geodesy, 2017.
[13] A. Kleusberg, and , P.J.G. Teunissen (Eds), "GPS for Geodesy, " 2nd Edition, Springer-Verlag, Berlin, 1998.
[14] R. Dach, , U. Hugentobler, P. Fridez, M. Meindl, "Bernese GPS Software Version 5.0", Astronomical Institute, University of Berne (AIUB), 2007
[15] C. Brunini and F. Azpilicueta, "GPS slant total electron content accuracy using the single layer model under different geomagnetic regions and ionospheric conditions," Journal of Geodesy, vol. 84, pp. 293-304, 2010.
[16] C. Brunini and F. J. Azpilicueta, "Accuracy assessment of the GPS-based slant total electron content," Journal of Geodesy, vol. 83, pp. 773-785, 2009.
[17] MGEX-DCB. ftp://cddis.gsfc.nasa.gov/gps/products/mgex/dcb/ .Accessed on January 1st, 2018.
[18] BKG, Agency for Cartography and Geodesy, ftp://igs.bkg.bund.de/. Accessed on January 1st, 2018.
[19] OMNIWeb, http://omniweb.gsfc.nasa.gov/form/dx1.html. Accessed on January 1st, 2018.
[20] MGEX, IGS Multi-GNSS Experiment. ftp://cddis.gsfc. nasa. gov /gps/products/mgex. Accessed on January 1st, 2018.